frontiers in Water

TYPE Original Research
PUBLISHED 11 June 2026
DOI 10.3389/frwa.2026.1840091

OPEN ACCESS

EDITED BY
Michelle E. Newcomer,
Berkeley Lab (DOE), United States

REVIEWED BY
Michael Tso,
UK Centre for Ecology and Hydrology (UKCEH), United Kingdom
Xi Zhu,
Chinese Academy of Sciences, China

*CORRESPONDENCE
Menberu B. Meles
✉ menberu.meles@usda.gov

RECEIVED 26 March 2026
REVISED 24 April 2026
ACCEPTED 27 April 2026
PUBLISHED 11 June 2026

CITATION
Meles MB, Raulerson S, Rau B, Rahman M and Jackson CR (2026) New metrics for characterizing and comparing soil moisture dynamics across depths and locations. *Front. Water* 8:1840091. doi: 10.3389/frwa.2026.1840091

New metrics for characterizing and comparing soil moisture dynamics across depths and locations

Menberu B. Meles[1]*, Scott Raulerson[2], Benjamin Rau[3], Mashrekur Rahman[1] and C. Rhett Jackson[2]

[1]USDA, ARS, Sustainable Agricultural Water Systems Unit, Davis, CA, United States, [2]Warnell School of Forestry and Natural Resources, University of Georgia, Athens, GA, United States, [3]Timber and Watershed Laboratory, USDA Forest Service, Northern Research Station, Parsons, WV, United States

Soil moisture dynamics play a crucial role in hydrological and agroecological processes, yet currently, there are few viable statistical procedures readily available to compare soil moisture time series data from multiple locations or soil horizons. We introduce three novel soil moisture time series signatures to characterize and compare soil moisture dynamics across depths and locations: (1) recession slope, (2) slope reversal frequency, and (3) soil moisture flashiness index. We calculated two recession slopes, one between saturation and field capacity and a second between field capacity and wilting point. We applied these metrics to in-situ soil moisture data taken at different depths and locations within five experimental watersheds across the United States varying in climate and vegetation. Results show that recession slopes generally decrease with depth, with surface layers exhibiting 2–3 times steeper recessions than deeper layers. Slope reversal frequency and flashiness also decrease with depth, reflecting the damping of wetting fronts. Flashiness was strongly tied to climate and showed inter-annual variability. These signatures effectively capture the integrated effects of climate, soil properties, and landscape position on soil moisture dynamics. Our findings demonstrate the potential of these metrics for improving landscape characterization, drought prediction, and understanding of hydrological and ecological processes across diverse environments.

KEYWORDS
integrated soil moisture control, slope reversal frequency, soil moisture dynamics, soil moisture flashiness, soil moisture recession slope

Highlights

- New soil moisture signatures capture rate of moisture loss, slope reversals, and flashiness.
- The signatures exhibited significant variability across space, time, and depth.
- The metrics quantify depth-dependent damping of soil moisture dynamics and reveal strong climatic controls on flashiness.
- The signatures effectively integrate effects of morphology, soil, climate, and land cover on moisture variability.

1 Introduction

Soil moisture is a critical driver of hydrological and agroecological processes, influencing runoff generation, primary production, drought susceptibility, and biogeochemical cycling (Western et al., 2004; Vereecken et al., 2008; Seneviratne et al., 2010). Understanding and predicting soil moisture dynamics across landscapes is crucial for water resource management, agricultural planning, and ecosystem assessment (Robinson et al., 2008; Famiglietti et al., 2008). However, characterizing soil moisture variability remains challenging due to the complex interactions between climate, soil properties, topography, and vegetation (Wilson et al., 2004; Famiglietti et al., 2008; Crow et al., 2012; Kathuria et al., 2019).

Traditional approaches to characterizing soil moisture variability have focused on spatial patterns of mean moisture content or total storage (Robinson et al., 2008; Fern'andez-Long et al., 2021; Brocca et al., 2007; Vereecken et al., 2014). Other methods for characterizing soil moisture rely on topographic indices, such as the Topographic Wetness Index (Sörensen et al., 2006) or its variants (Kopecỳ et al., 2021; Riihimäki et al., 2021; Meles et al., 2020; Radu-la et al., 2018; Larson et al., 2022). While useful, these approaches have limited predictive capability due to oversimplified assumptions and coarse input data (Grabs et al., 2009; Meles et al., 2020; Buchanan et al., 2014).

Recent studies have begun to explore the temporal dynamics of soil moisture to better understand landscape-scale hydrological processes (Grayson et al., 1997; Corradini, 2014; Penna et al., 2013; Kim, 2016; Mittelbach and Seneviratne, 2012). Most of these efforts have focused on event-based responses or seasonal patterns, rather than characterizing the overall behavior of soil moisture time series. Some recent studies have attempted to derive hydrological signatures from soil moisture data (Branger and McMillan, 2020; Araki et al., 2022; Addor et al., 2018), but there remains a need for metrics that can effectively capture the complex dynamics of soil moisture across different depths and locations.

The temporal variability of soil moisture plays a crucial role in various ecological and hydrological processes. For instance, Entekhabi et al. (1996) demonstrated the importance of soil moisture dynamics in land-atmosphere feedback mechanisms and regional climate regulation. This work has been further developed by Seneviratne et al. (2010) and Koster et al. (2004), who highlighted the role of soil moisture in climate variability and predictability. Kim (2009) and Famiglietti et al. (2008) emphasized the influence of soil moisture temporal dynamics on vegetation-soil interactions, transpiration, and drainage processes. Soil moisture dynamics are a key driver of wildfire ignition and spread (Holden et al., 2025), and have been intrinsically linked to multiple other ecosystem functions in diverse geographical and climatic conditions (Löffler, 2007; Xu et al., 2022; Collison et al., 2013; Hamerlynck et al., 2012).

Verrot and Destouni (2016) emphasized the importance of long-term soil moisture time series in evaluating land surface hydrologic models. This has been complemented by studies on the use of soil moisture data in improving streamflow forecasts (Koster et al., 2010) and climate predictions (Seneviratne et al., 2013). Drydown analysis characterizes soil moisture loss between rainfall events as an exponential decay process, capturing post-wetting persistence and memory (Shellito et al., 2016; McColl et al., 2017; Tso et al., 2023; Araki et al., 2022). It represents the full drying period and integrates drainage and atmospheric demand into a single decay timescale (τ), without requiring explicit identification of field capacity. Most applications focus on near-surface soil moisture (~5 cm), where the lag between rainfall and peak response is small, allowing precipitation timing to define drydown onset. At greater depths, however, this lag becomes more variable, complicating precipitation-based event identification. Tso et al. (2023) addressed this by adopting a soil-moisture-only approach identifying consecutive periods of monotonically decreasing soil moisture independent of rainfall applied to depth-integrated COSMOS-UK observations (0–80 cm, surface-weighted). Extending drydown analysis to depth-resolved and remotely sensed datasets offers new opportunities to study soil moisture dynamics across scales, though challenges remain in reconciling these with in situ observations (e.g., Crow et al., 2012; Mohanty et al., 2017; Araki et al., 2022). The recession slope framework introduced here follows a similar soil-moisture-only philosophy, enabling depth-resolved drying characterization across contrasting soils and landscapes.

Despite these advancements, a gap remains in our ability to quantitatively compare soil moisture behavior across sites, depths, and landscape positions, highlighting the need for metrics by which to characterize soil moisture time series. Current methods often fail to capture the integrated effects of various biotic and abiotic factors that control soil moisture dynamics (Vereecken et al., 2014; Robinson et al., 2008; Mohanty et al., 2017). Simple summary statistics, such as mean or total volumetric soil water content, are generally insufficient for interpreting complex hydrologic processes at hillslope and catchment scales, due to high temporal variability and the non-stationary nature of most systems. These limitations hinder our understanding of how soil moisture responds to climate variability and land-use changes across diverse environments (Famiglietti et al., 2008; Teuling et al., 2007; Mimeau et al., 2021). Despite these advancements, a gap remains in our ability to quantitatively compare soil moisture behavior across sites, depths, and landscape positions, highlighting the need for robust metrics to characterize soil moisture time series.

In this study, we propose three novel soil moisture time series signatures that integrate the complex interactions of biotic and abiotic factors controlling soil moisture dynamics:

1. *Recession slope*: The rate of soil moisture loss between rainfall events
2. *Slope reversal frequency*: The number of times soil moisture content increases to a peak and then decreases over a given time period
3. *Soil matrix flashiness index*: A measure of the frequency and rapidity of short-term changes in soil moisture content

These signatures build upon concepts from stream hydrology (e.g., recession analysis and flashiness indices) (Brutsaert, 2008; Baker et al., 2004) but are adapted to the unique characteristics of soil moisture time series in such a way they provide complementary and non-redundant characterizations of soil moisture dynamics. By analyzing these signatures across depths and locations, we aim to provide new insights into the factors controlling soil moisture dynamics and their implications for hydrological and ecological processes.

The objectives of this study are to:

1. Define and calculate the proposed soil moisture time series signatures using in-situ data from five experimental watersheds across the United States.

2 Compare these signatures across various depths (0–10, 25–30, 35–45, and 50–60 cm) and locations to evaluate soil moisture dynamics between rainfall events.
3 Assess the relationships between the new signatures and soil properties, such as porosity, to better understand the physical controls on soil moisture behavior.

By introducing these new metrics, we aim to provide researchers and practitioners with quantitative tools for comparing soil moisture behavior across sites, soil types, depths, and landscape positions. These signatures have the potential to improve our understanding of drought sensitivity (Sheffield et al., 2012; AghaKouchak et al., 2015), water use efficiency (Hatfield et al., 2001; Molden et al., 2010), and ecosystem functioning (Rodr'ıguez-Iturbe and Porporato, 2007; D'Odorico et al., 2010) across diverse environ- ments. Furthermore, they may enhance our ability to predict hydrological responses to climate change (Seneviratne et al., 2013), land-use modifications (Robinson et al., 2008; Penna et al., 2013), and even improve our understanding of human-drought interactions (Rahman et al., 2024), thereby supporting more effective water resource management and conservation strategies.

This research builds upon recent efforts to derive meaningful hydrological signatures from soil moisture data (Araki et al., 2022; Branger and McMillan, 2020; Shellito et al., 2016; McColl et al., 2017) and extends these approaches to capture the full complexity of soil moisture dynamics across different spatial and temporal scales. By providing a comprehensive analysis of soil moisture time series characteristics, our study contributes to the growing body of research aimed at improving landscape characterization and hydrological process understanding (Carra˜o et al., 2016; Kim, 2016; Verrot and Destouni, 2016; Vereecken et al., 2014; Robinson et al., 2008).

2 Materials and methods

2.1 Study sites and data collection

This study utilized in-situ soil moisture data from five experimental watersheds across the United States, representing a diverse range of climatic, topographic, and ecological conditions (Figure 1). Table 1 summarizes the key characteristics of the soil moisture datasets used in this study. A persistent challenge in multi-site soil moisture analysis is that data collection protocols vary substantially across observational networks, as reflected in Table 1. Measurement depths, sensor types, temporal resolution, and record duration all differ across the five sites, and such non-uniformity is likely to remain a practical reality in soil moisture research for the foreseeable future as a challenge for regional to large-scale analyses.

To enable structured cross-site comparison, observation depths were grouped into four approximate categories: surface (~5 cm), shallow (~25–30 cm), intermediate (~45 cm), and deep (~50–60 cm). This classification enables consistent interpretation across sites while retaining the ability to account for site-specific characteristics where necessary. Additionally, known sensor-specific limitations such as the thermal lag associated with heat dissipation sensors at Oklahoma Mesonet sites may affect the computed signatures. Together, these factors underscore the importance of site-aware interpretation when analyzing multi-site soil moisture data. A detailed description of the study sites, each providing unique insights into soil moisture dynamics under varying environmental conditions, is provided below.

2.1.1 Little Washita experimental watershed

Located in southwestern Oklahoma (34.957° N, −97.935° W), this 610 km^2 watershed is characterized by rolling topography (mean slope ~2%) with land cover dominated by rangeland and cropland

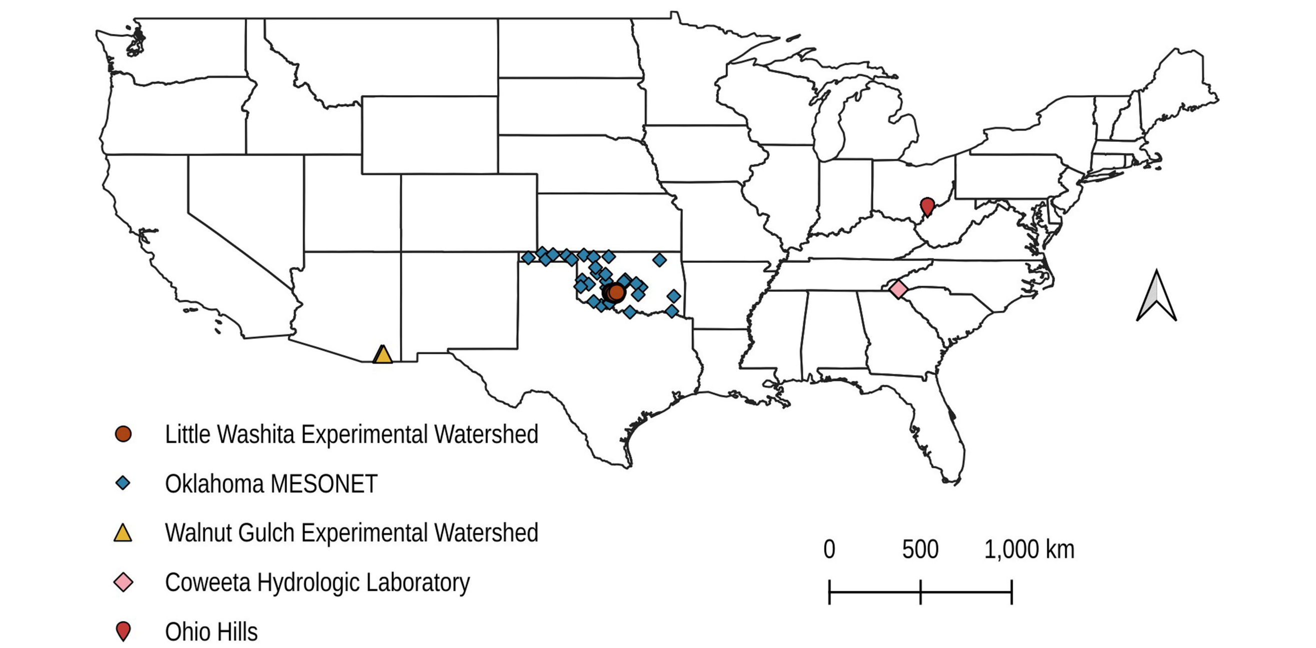

FIGURE 1
Map of CONUS showing locations of study sites: (1) Little Washita, (2) Oklahoma MESONET, (3) Walnut Gulch, (4) Coweeta, and (5) Ohio Hills.

TABLE 1 Characteristics of sub-daily in-situ soil moisture datasets from five experimental watersheds.

Site	Number of locations	Measurement depths (cm)	Data duration (years)	Sensor type	Climate classification
Little Washita	29	5, 25, 45	25	Stevens Hydra Probe	Sub-humid continental
Oklahoma MESONET	30	5, 25, 60	21	CSI 229-L heat-dissipation	Various
Walnut Gulch	12	5, 30, 50	3	ECH2O EC-5	Semi-arid
Coweeta	15	30, 60	6	Campbell Scientific CS615 EC	Humid subtropical
Ohio Hills	18	60	8	ECH2O EC-5	Humid continental

(Cosh et al., 2006). The site experiences a sub-humid continental climate with average annual precipitation of 760 mm and an average annual temperature of 16 °C (Starks et al., 2014a, 2014b). Soil textures vary from fine sand to silty loam, with moisture monitoring utilizing automated electromagnetic sensors (e.g., Stevens Water Hydra Probes) at multiple depths to capture profile-scale dynamics (Cosh et al., 2006; Starks et al., 2014a, 2014b). The area is characterized by complex pedon stratigraphy, including clay-rich argillic horizons that significantly influences drainage and moisture retention (Wilson et al., 2004; Heathman et al., 2003). Vegetation is grassland and rangeland with mixed agricultural and isolated forest areas.

2.1.2 Walnut Gulch experimental watershed

Situated near Tombstone, Arizona (31.72° N, −110.35° W), this 150 km^2 semi-arid watershed with average annual precipitation of 312–350 mm, an average annual temperature of 17.7 °C. And with elevation ranging from 1,200 to 1950 m (Moran et al., 2008). The study focused on the Lucky Hills and Kendall sub-basins, each less than 0.1 km^2. Soils are predominantly characterized by alluvial sandy with slopes 2–3% in Kendall and are dominated by loamy sand mixed with stones with 4–9% slopes in Lucky Hills (Heilman et al., 2008). Vegetation varies from shrub-dominated (Lucky Hills) to grass-dominated (Kendall).

2.1.3 Oklahoma Mesonet

This network comprises over 115 automated stations covering approximately 181,000 km^2 in the US state of Oklahoma (McPherson et al., 2007). For this study, we selected 30 locations based on the exhibited soil moisture dynamics. The network spans various climate and vegetation zones within Oklahoma. The sites have significant precipitation gradient ranging from 430 mm to 1,420 mm and temperature range from 13.3–16.7 °C. The Oklahoma Mesonet primarily uses Campbell Scientific 229-L (CSI 229-L) heat dissipation sensors (HDS) to monitor soil moisture across its network (Illston et al., 2008; Scott et al., 2013). These sensors are valued for their durability and wide measurement range for soil matric potential—the capillary force required to retain water in soil (Basara and Crawford, 2000; Illston et al., 2008). Because HDS infer moisture from the thermal response of a porous ceramic element to a heat pulse, they exhibit a known physical and thermal lag, particularly during rapid wetting events (Basara and Crawford, 2000; Cook, 2016).

2.1.4 Coweeta hydrologic laboratory

Located in the Appalachian oak section of the Mesophytic forest region (35.058° N, −83.435° W), this site provided data from 15 stations (Dyer, 2009). The humid subtropical climate supports high annual precipitation ranging from 1800 mm in lower elevation to 2,300 mm in higher elevation and mean annual temperature ≈ 12.5–13 °C. Elevation ranges from 685 m to ~1,600 m with generally steep slope above 30%. Monitoring at the site primarily utilizing time-domain reflectometry (TDR) sensors and tensiometers to measure soil water potential and moisture content (Hales and Miniat, 2017). Pedon descriptions indicate deep, well-drained soils with loamy to sandy loam textures, high hydraulic conductivity, and thick organic O-horizons (USDA NRCS, 2019). These pedon-specific infiltration capacities and highly weathered saprolite layers are essential for modeling the watershed's rapid response to storm events (Hewlett and Hibbert, 1963).

2.1.5 Ohio Hills

Situated in the Ohio Allegheny Plateau, USA (39.27° N, −81.96° W), the Ohi Hills site is characterized by moderate relief with elevation range from 675 to 980 m. The climate is humid continental, with average annual precipitation of 1,006 mm and an average annual temperature of 11 °C (Dyer, 2006, 2009). The watershed is predominantly forested and specifically characterized by temperate deciduous (mesophytic) forest cover. Average hillslope gradients range between 5 and 6%. Soils developed under these forested conditions exhibit increasing clay content with depth, resulting in reduced macroporosity and lower saturated hydraulic conductivity in subsoil horizons. Consequently, topographic control on soil moisture decreases with depth, reflecting stronger vertical impedance to flow and enhanced subsurface water retention in deeper layers.

2.2 Data preprocessing and quality control

Raw soil moisture data were subjected to quality control procedures to remove erroneous readings and fill data gaps. We applied the following steps:

1. Removal of physically implausible values (e.g., volumetric water content > porosity or < 0)
2. Identification and removal of outliers using the Interquartile Range (IQR) method
3. Gap-filling for short periods (less than 12 h) using linear interpolation
4. Data were homogenized to a common temporal resolution (hourly) across all sites, as most observations were already available at this timestep. This standardization also helps reduce high-frequency sensor noise, such as the amplified short-term variability observed in the Oklahoma Mesonet dataset.

5 The soil moisture observations were converted to volumetric soil moisture content across the study sites. For example, soil matric potential measurements from the Oklahoma Mesonet data were converted to volumetric soil moisture content using the method described by Illston et al. (2008).

The hourly homogenization was adopted based on the temporal resolution of the available data and the broader objective of understanding site properties across depth. Gap filling was applied only to short gaps—specifically, those shorter than 12 consecutive hours and was limited to portions of the time series with near-complete records and minimal missing data. Periods characterized by longer or more frequent gaps were excluded entirely from signature computation rather than being filled (e.g., segments of the Walnut Gulch dataset) to minimize the artificial smoothed interpolated segments.

2.3 Soil moisture time series signatures

We developed three novel soil moisture time series signatures to characterize the dynamic behavior of soil moisture. Although all three signatures characterize aspects of soil moisture temporal dynamics, they capture fundamentally different and complementary dimensions of system behavior (Figure 2).

2.3.1 Recession slope

The recession slope quantifies the rate of soil moisture loss between rainfall events, approximated linearly with a breakpoint at field capacity, and reflects the integrated influence of soil physical properties (e.g., texture, porosity, hydraulic conductivity), geomorphic setting (e.g., slope position, contributing area, subsurface connectivity), and atmospheric demand (e.g., evapotranspiration, vapor pressure deficit). As such, it captures the full spectrum of factors that regulate how quickly a soil profile drains and dries following a wetting event. The workflow analyzes hourly soil-moisture time-series data to quantify wetting and drying dynamics between rainfall events. The data are first smoothed using a rolling average to reduce high-frequency noise. Peak-detection algorithms are then applied to identify local maxima corresponding to post-rainfall soil-moisture peaks and the preceding local minima as the water content approaches the wilting point representing pre-event baseline conditions.

For each valley–peak pair, characteristic time intervals are defined, including the total event duration, the rapid wetting period, and the post-event recession period. Soil-moisture thresholds corresponding to saturation, field capacity (fc), and wilting point (wp) are used to quantify moisture gains and losses during these phases.

Saturation and wilting point thresholds were defined empirically for each soil moisture time series, with additional guidance from pedon data. Saturation was approximated as the 95th and 5th percentile (or, in some cases, the 90th and 10th percentile) of observed volumetric water content, reflecting the upper and lower envelope of moisture states achieved at each location and depth. This choice accounts for variability under near saturated and dry conditions but requires careful consideration to ensure consistency across sites. Site-specific flexibility, especially in wilting point estimation, was necessary because many time series, particularly deeper depths or wetter sites rarely reach true residual moisture conditions, making fixed lower percentiles unreliable.

Field capacity was identified separately for each time series (i.e., by location and depth) using a combination of approaches informed by site characteristics and available pedon information. It is defined as the inflection point on the soil-moisture recession curve, marking the transition from rapid gravitational drainage to slower, retention-controlled moisture loss. Specifically, field capacity was determined as the point of maximum curvature change along the recession limb, consistent with its physical definition as the moisture content at which

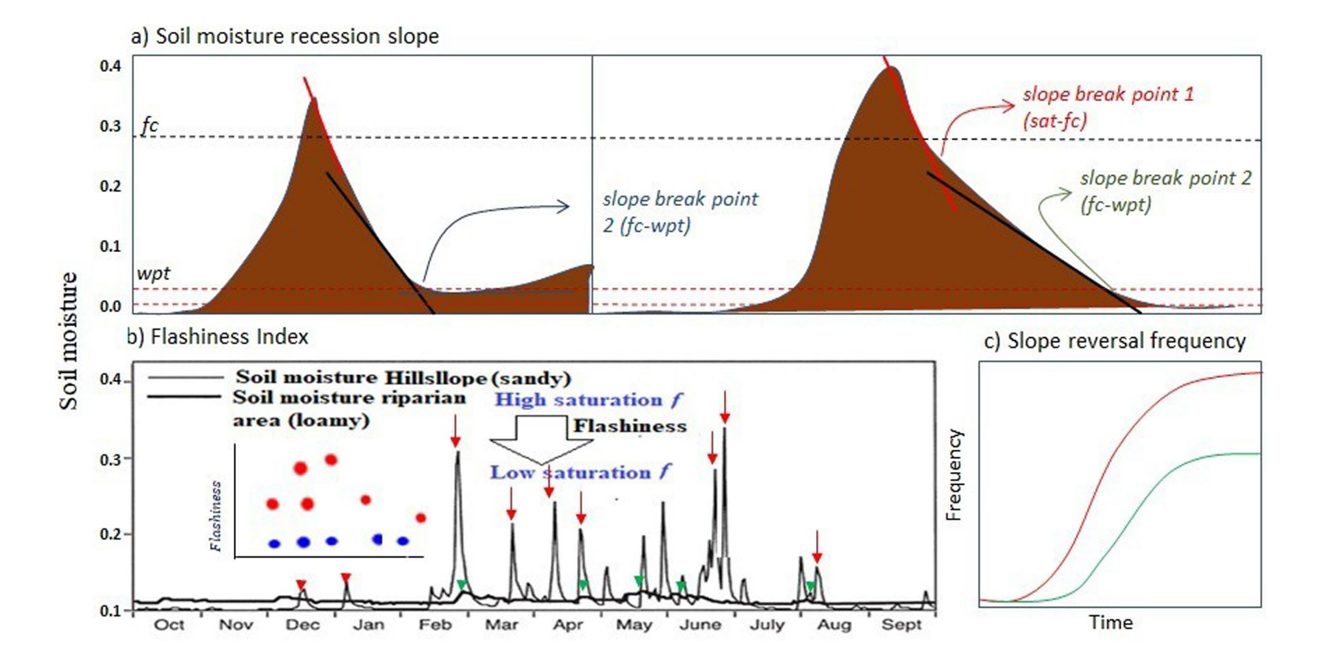

FIGURE 2
The proposed soil moisture signatures that integrated the various factors affecting soil moisture dynamics: **(a)** The soil moisture recession slopes between the rainfall events, **(b)** the soil matrix flashiness index, and **(c)** the cumulative soil moisture slope reversal frequency.

gravitational drainage becomes negligible relative to capillary retention forces. Identification relied on visual inspection, which, although time-consuming, provides robust interpretation; however, we acknowledge that this approach introduces some site- and depth-specific subjectivity, particularly where recession curves are gradual or noisy.

To characterize soil hydraulic behavior, two recession slopes are calculated:

$$Slope-1=\frac{\mathrm{sm}_{sat,t}-\mathrm{sm}_{fc,t}}{\Delta t} \tag{1}$$

$$Slope-2=\frac{\mathrm{sm}_{fc,t}-\mathrm{sm}_{wp,t}}{\Delta t} \tag{2}$$

Where $\mathrm{sm}_{\mathrm{sat}}$, $\mathrm{sm}_{\mathrm{fc}}$, and $\mathrm{sm}_{\mathrm{wp}}$ represent soil moisture at saturation, field capacity, and wilting point, respectively, and Δt is the time difference between corresponding soil moisture values. Slope-1 (Equation 1) represents the rapid drainage of gravitational water immediately following saturation, while Slope-2 (Equation 2) characterizes slower moisture loss governed by drainage and evapotranspiration processes. Comparisons across depths, events, and locations indicate that steeper slopes correspond to faster moisture redistribution, whereas gentler slopes reflect stronger soil water retention.

In contrast to the exponential drydown framework (Shellito et al., 2016; McColl et al., 2017), which represents the post-rainfall drying period using a single decay curve and associated timescale (τ), the Slope-1 and Slope-2 approach explicitly distinguishes between gravitational drainage above field capacity and retention-controlled moisture loss at lower moisture states. This separation captures temporal variability in soil moisture dynamics and reflects the combined influence of both dynamic (e.g., atmospheric demand) and static (e.g., soil properties) controls.

2.3.2 Slope reversal frequency

Slope Reversal Frequency (SRF) quantifies the number of wetting–drying transitions in volumetric soil moisture, defined as increases to a local peak followed by decreases that fall below the wilting-point threshold, normalized by the total analysis period:

$$SRF=\frac{\mathrm{N}_{reversal}}{T} \tag{3}$$

Where $N_{\mathrm{reversals}}$ is the number of slope reversals and T is the total time period in days. Higher SRF values indicate more frequent wetting–drying cycles.

The SRF (Equation 3) quantifies the number of discrete wetting-drying transitions that exceed a defined threshold (e.g., wilting point), providing a dynamic complement to the Slope-1 and Slope-2 metrics. Specifically, it reflects the interaction between precipitation frequency and intensity and the soil's ability to transition between rapid drainage (Slope-1-dominated) and slower, retention-controlled drying (Slope-2-dominated) regimes. Environments with frequent rainfall and well-drained soils tend to exhibit high reversal frequencies due to repeated switching between these regimes. In contrast, arid and semi-arid regions, where rainfall events are infrequent, show fewer reversals regardless of soil properties. Similarly, soils with limited drainage capacity or those sustained by persistent moisture inputs tend to remain within a single regime for longer periods, resulting in fewer reversals even under frequent precipitation. In this sense, SRF serves as a single metric that integrates climatic forcing with vadose zone response, linking the timing of wetting-drying transitions to the process-based insights provided by the Slope-1/Slope-2 framework.

2.3.3 Soil matrix flashiness index

The Soil Matrix Flashiness Index (SMFI; Equation 4) quantifies short-term variability in soil-moisture storage by measuring the cumulative magnitude of successive changes in soil moisture relative to total moisture content. Unlike slope reversal frequency, which relies on threshold crossings or discrete event identification, SMFI captures continuous variability in the soil moisture signal, regardless of whether a full wetting–drying cycle occurs. Slope reversal frequency counts how often the soil moisture system is reset by rainfall, whereas flashiness measures the aggregate intensity of all fluctuations, including minor oscillations that do not reach saturation or drop to the wilting point. We adapted the Richards-Baker Flashiness Index (Baker et al., 2004) for soil moisture time series:

$$R-B\ Index=\frac{\sum_{t=1}^{n}\left|\mathrm{q}_{t-1}-q_t\right|}{\sum_{t=1}^{n}\mathrm{q}_t} \tag{4}$$

Where q_t is the soil moisture content at time t, and n is the number of observations. Higher R values indicate more rapid soil-moisture fluctuations, while lower values indicate more stable, buffered soil-moisture conditions.

Figure 2 illustrates these three soil moisture signatures and how they capture different aspects of soil moisture dynamics. Together, they provide complementary and non-redundant characterizations of soil moisture dynamics: the rate of moisture loss, the frequency of threshold-crossing cycles, and the cumulative energy of continuous fluctuations.

3 Results

3.1 Moisture recession slopes

Computed recession slopes exhibited substantial variability across depths, locations, and sites (Figures 3–5). Across all datasets, recession slopes calculated between saturation and field capacity (Slope-1) consistently exceed slopes calculated between field capacity and wilting point (Slope-2) and is in the range of a factor of two to three. This shows the gravity-drainage vs. retention-controlled dynamic that explains the two slopes.

Both recession slopes generally decreased with depth (Figure 3; Table 2), with the shallowest observation depths (5–10 cm) exhibiting the largest magnitudes and greatest variability (Table 2). Deeper layers (50–60 cm) showed gentler and more consistent recession behavior, while intermediate depths (25–45 cm) displayed transitional patterns with site-specific deviations from monotonic depth trends. For example, at Walnut Gulch and the Oklahoma Mesonet, recession slopes at 50–60 cm were comparable to or greater than those at 25–30 cm. At

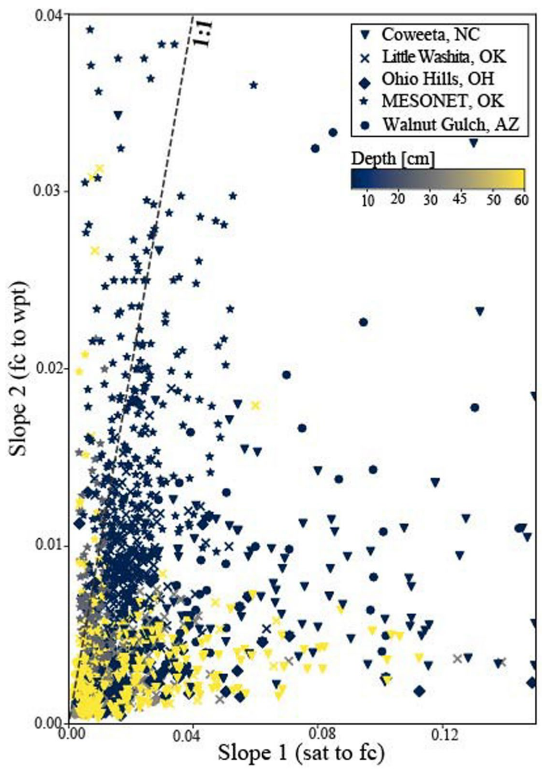

FIGURE 3
The distribution of slope 1 (x-axis) and slope 2 (y-axis) for all sites, locations, and depths of soil moisture time series. Soil moisture loss rate at the surface is steeper and highly variable. The scatter plot colors represents depth of in-situ soil moisture observations from shallow (blue) to deeper depths (yellow).

Walnut Gulch, this pattern is likely related to high aridity, whereas at Oklahoma Mesonet sites the heat dissipation sensor method has known limitations in capturing short-term soil-moisture dynamics following rainfall events. Oklahoma Mesonet sites also showed relatively high recession slopes with stronger correspondence between Slope-1 and Slope-2.

Across sites (Figures 4, 5), humid locations (e.g., Coweeta) exhibited broader distributions of recession slopes, whereas semi-arid sites (e.g., Walnut Gulch) showed narrower ranges (see Table 2). Within individual sites, recession slopes varied among locations (Figure 5b), indicating substantial spatial heterogeneity in soil-moisture loss behavior under similar climatic forcing. This pattern is illustrated at the Kendall site, where locations on the northeastern side of the watershed, characterized by alluvial sandy soils and grass cover, exhibited greater variability and steeper recession slopes than those at the Lucky Hills site, which is dominated by loamy sand with stones and brush cover. These differences in computed slope values highlight the combined influence of vegetation cover, soil type, and topographic setting.

3.2 Slope reversal frequency

Slope reversal frequency generally decreased with depth across most sites (Figures 6c,d), with surface layers exhibiting the highest frequency of wetting–drying transitions. Deeper layers showed fewer reversals and smoother temporal behavior, reflecting the damping and merging of wetting fronts with depth, consistent with observations by McColl et al. (2017).

Across locations, slope reversal frequency varied with site and depth but scaled consistently with saturated volumetric water content. Sites with higher maximum soil moisture tended to exhibit higher reversal frequencies, particularly in surface layers (Figures 6c,d). At Walnut Gulch (Figure 6a), strong contrasts were observed between shallow and deeper layers, with minimal reversal activity below the surface due to high temperatures and evaporative demand. Under these conditions, soil moisture in surface layers is rapidly lost to evaporation (e.g., Seneviratne et al., 2010; Goodrich et al., 2008), limiting moisture recharge to deeper layers under low rainfall and dry antecedent conditions.

Temporal aggregation of reversal counts (Figures 6a,b) showed greater variability at shallow depths and more stable behavior at depth, depending on the presence of restrictive layers and textural contrasts. These depth-dependent patterns were consistent across sites with multi-depth measurements (e.g., McColl et al., 2017).

The strength of the depth dependence varied between locations at Little Washita (Figures 6a,b) and between Little Washita and Walnut Gulch (Figures 6c,d), likely reflecting differences in precipitation regimes and atmospheric evaporative demand (Seneviratne et al., 2010).

Soils with higher porosity, approximated by maximum volumetric water content and typically associated with higher hydraulic conductivity, tended to exhibit higher slope reversal frequencies (Figures 6c,d), consistent with the role of soil texture in controlling soil-moisture dynamics (McColl et al., 2017).

3.3 Soil matrix flashiness

The adapted Richards–Baker flashiness index exhibited clear depth dependence, with the highest values occurring near the surface and decreasing with depth (Figure 7). Surface layers also showed greater interannual variability in flashiness compared to deeper layers.

Flashiness varied across sites, with Little Washita exhibiting pronounced interannual variability and Walnut Gulch showing relatively stable values across years. Across locations, flashiness generally decreased with increasing saturated volumetric water content (porosity), with less conductive soils tending to exhibit higher flashiness values (e.g., Garcıa et al., 2014). Reduced downward water movement due to evaporation further contributed to decreasing flashiness with depth.

Interannual variability in flashiness was substantial at Little Washita but minimal at Walnut Gulch (Figure 7), likely reflecting differences in the level of dynamics in the land use/cover condition and climatic conditions, consistent with the role of climate-driven variability in surface soil moisture dynamics reported by Seneviratne et al. (2010). The index was computed at daily resolution across all sites; comparisons are internally consistent but should be interpreted cautiously relative to values derived at other temporal resolutions.

4 Discussion and conclusion

The soil moisture signatures developed in this study: recession slopes, slope reversal frequency, and the soil moisture flashiness index provide quantifiable and reproducible metrics for comparing soil moisture dynamics across depths, sites, and landscape positions.

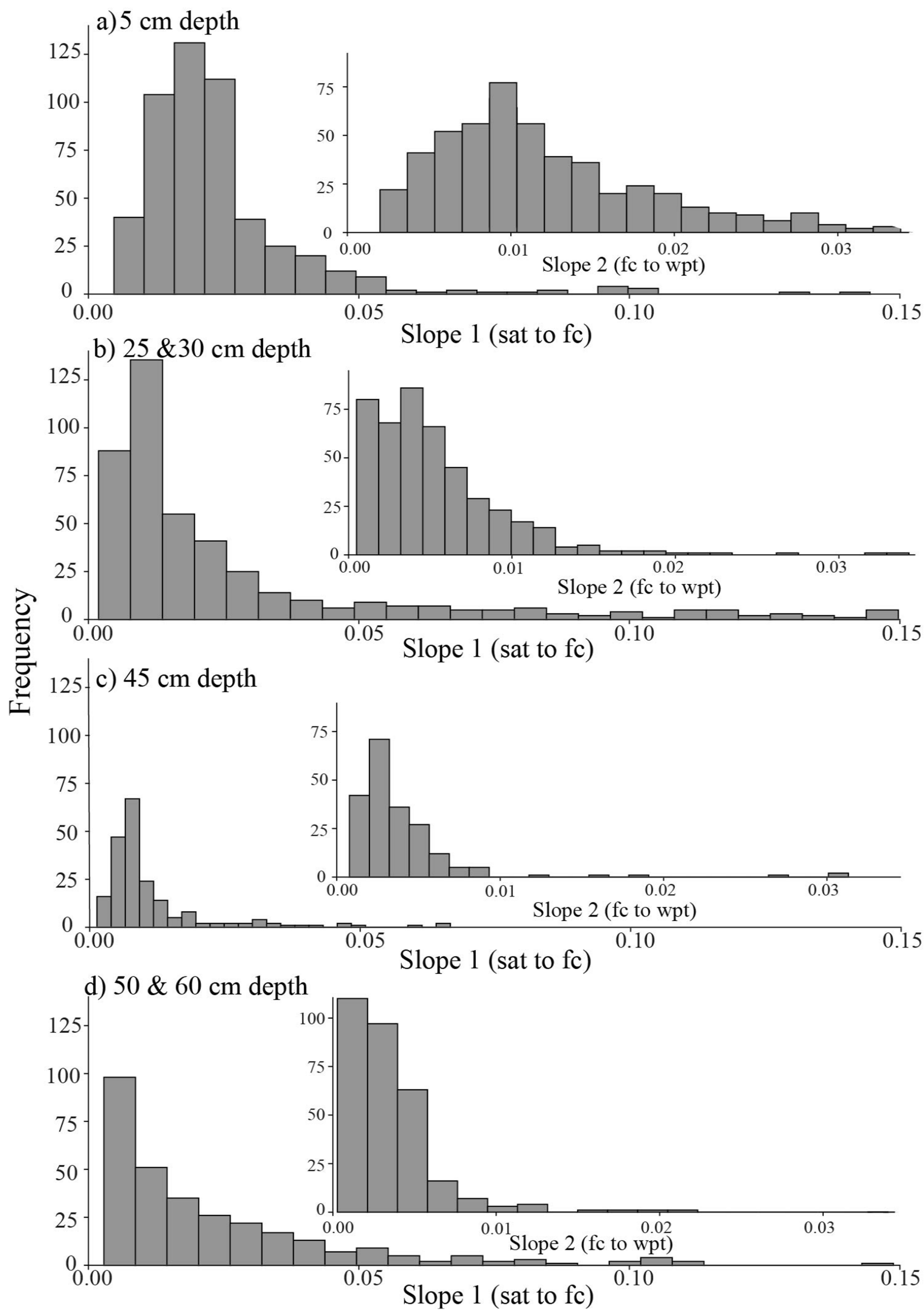

FIGURE 4
Frequency distribution of soil moisture loss rates (slopes) at different observation depths across all study sites: **(a)** 5 cm (note: no data available for Coweeta and Ohio Hills), **(b)** 25–30 cm, **(c)** 40–45 cm (data from Little Washita only), and **(d)** 50–60 cm. The in-set figure shows the distribution for slope 2 (field capacity to wilting point). Note that the *x*-axis scales differ substantially. Both slope-1 & slope-2 at 45 cm depth data represent Little Washita site only.

These signatures are computationally simple and rely solely on soil moisture time series, yet they capture systematic variability associated with hydrologic forcing and subsurface filtering processes. What we found regarding variability in soil moisture measurements was not surprising. The point is that these metrics can quantify the variability in important aspects of soil moisture dynamics.

Differences between recession slopes above and below field capacity reflect distinct moisture regimes within the soil profile. Steeper recession slopes between saturation and field capacity are consistent with gravity-dominated drainage and higher effective hydraulic conductivity under wet conditions, whereas gentler slopes below field capacity reflect reduced hydraulic connectivity and increasing control by soil water retention. The systematic decrease in recession slope magnitude with depth indicates attenuation of vertical drainage and reduced exposure to atmospheric demand, consistent with previous findings highlighting the influence of climate on soil moisture dynamics (McColl et al., 2017; Seneviratne et al., 2010). Deviations from monotonic depth trends at individual sites likely reflect soil profile

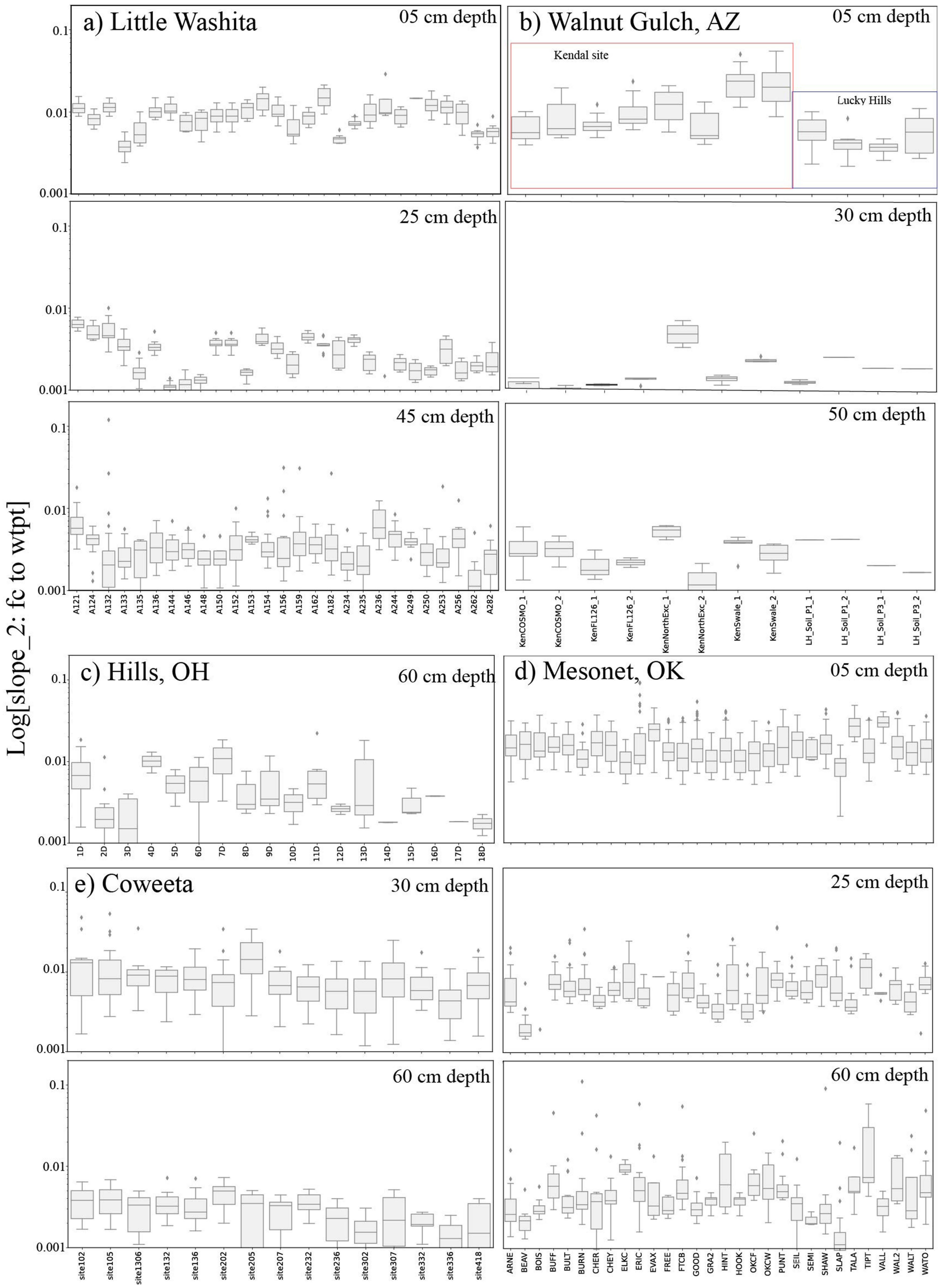

FIGURE 5
The distribution of slope 2 soil moisture recession rates across all locations and depths **(a)** Little Washita, **(b)** Walnut Gulch, **(c)** Ohio Hills, **(d)** OK Mesonet, and **(e)** Coweeta, NC. The whisker plot represents computed slope 2, while each panel represents different observation depths. Note Y-axis is given in log scales.

TABLE 2 Summary of median recession slope values with interquartile range (IQR) by site and depth.

Site	Depth	Slope-1 (sat to fc)		Slope-2 (fc to wpt)	
		Median	IQR	Median	IQR
Little Washita	~5 cm	0.0192	0.0087	0.0089	0.0037
	~25–30 cm	0.0123	0.0122	0.0027	0.0025
	~45 cm	0.0083	0.0062	0.0030	0.0024
Oklahoma Mesonet	~5 cm	0.0209	0.0125	0.0150	0.0098
	~25–30 cm	0.0076	0.0044	0.0060	0.0037
	~50–60 cm	0.0058	0.0031	0.0039	0.0032
Walnut Gulch	~5 cm	0.0293	0.0243	0.0055	0.0052
	~25–30 cm	0.0068	0.0083	0.0013	0.0014
	~50–60 cm	0.0046	0.0056	0.0025	0.0016
Coweeta	~25–30 cm	0.0381	0.0579	0.0063	0.0055
	~50–60 cm	0.0227	0.0264	0.0029	0.0023
Ohio Hills	~50–60 cm	0.0164	0.0248	0.0026	0.0025

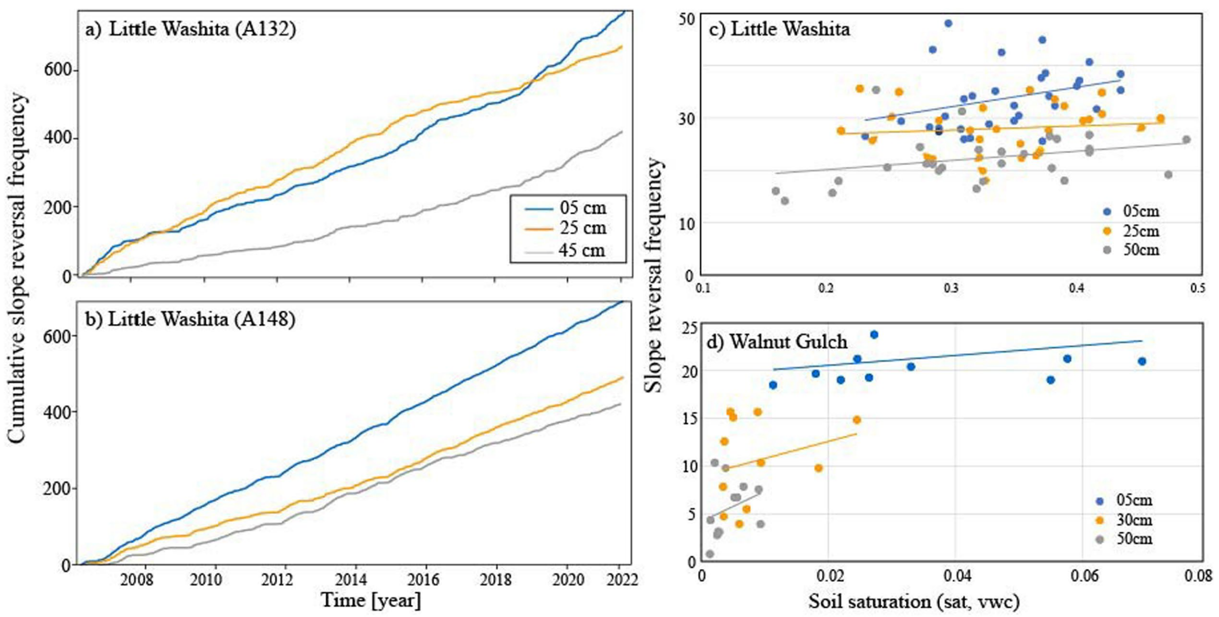

FIGURE 6
Cumulative slope reversal frequency at selected locations in Little Washita experimental watershed **(a,b)**. **(c,d)** Illustrate the distribution of the slope reversal frequency (number of reversals per year) with respect to the saturated volumetric water content for Little Washita **(c)** and Walnut Gulch **(d)**.

structure, hydraulic layering, or subsurface connectivity rather than climate alone.

Across sites, climate exerted a dominant first-order control on the magnitude and variability of all three signatures, particularly when contrasting humid and semi-arid environments. For example, high soil moisture loss rates at Walnut Gulch are consistent with its arid climate and high evaporative demand, whereas elevated loss rates at the steep, forested Coweeta site may reflect well-drained soils and topographic influences (Figures 8a,b). These patterns align with established relationships between topography, soil properties, and soil moisture dynamics (Famiglietti et al., 2008). At the same time, within-site variability in the signatures indicates that soil properties, vegetation cover, and landscape position modulate local soil moisture responses.

Slope reversal frequency captures temporal variability in soil moisture trajectories. Higher reversal frequencies near the surface are consistent with frequent wetting and drying cycles driven by precipitation inputs and evaporative losses, while decreasing reversal frequency with depth reflects damping of wetting fronts and integration of multiple surface events into smoother subsurface responses (Figure 8c). The association between reversal frequency and saturated volumetric water content suggests that storage capacity influences sensitivity to transient forcing. However, without explicit event attribution, reversals represent integrated system responses rather than discrete hydrological processes.

Flashiness reflects the cumulative magnitude of short-term soil moisture fluctuations and its behavior across climate regimes and

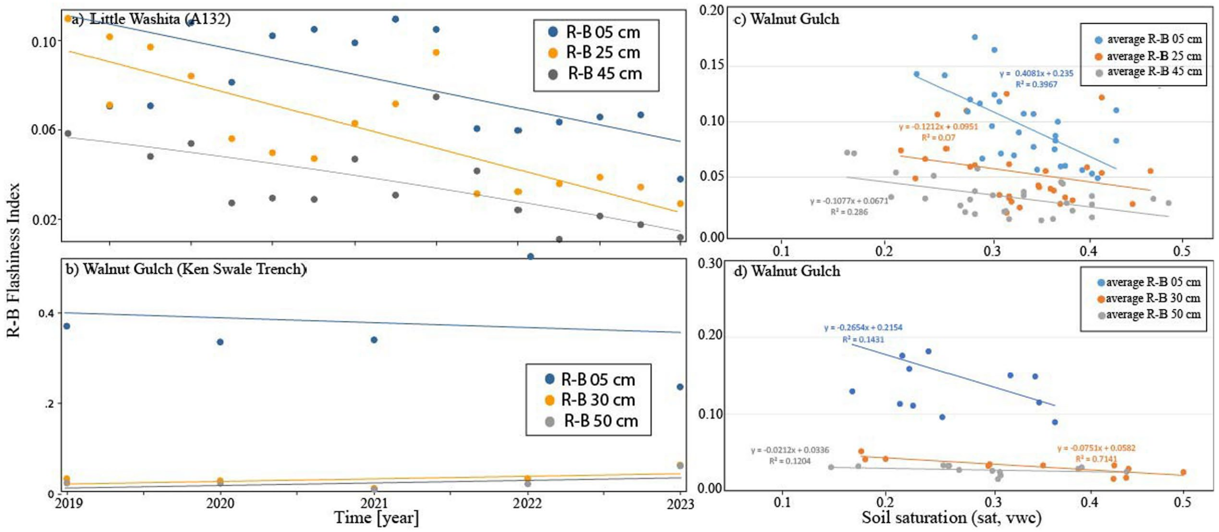

FIGURE 7
Left **(a,b)**: Interannual variation of the flashiness index (Richard-Baker) index computed at an annual scale for different depths at Little Washita and Walnut Gulch. Right **(c,d)**: The distribution of flashiness index with respect to the saturated volumetric water content for Walnut Gulch **(c)** and Little Washita **(d)**.

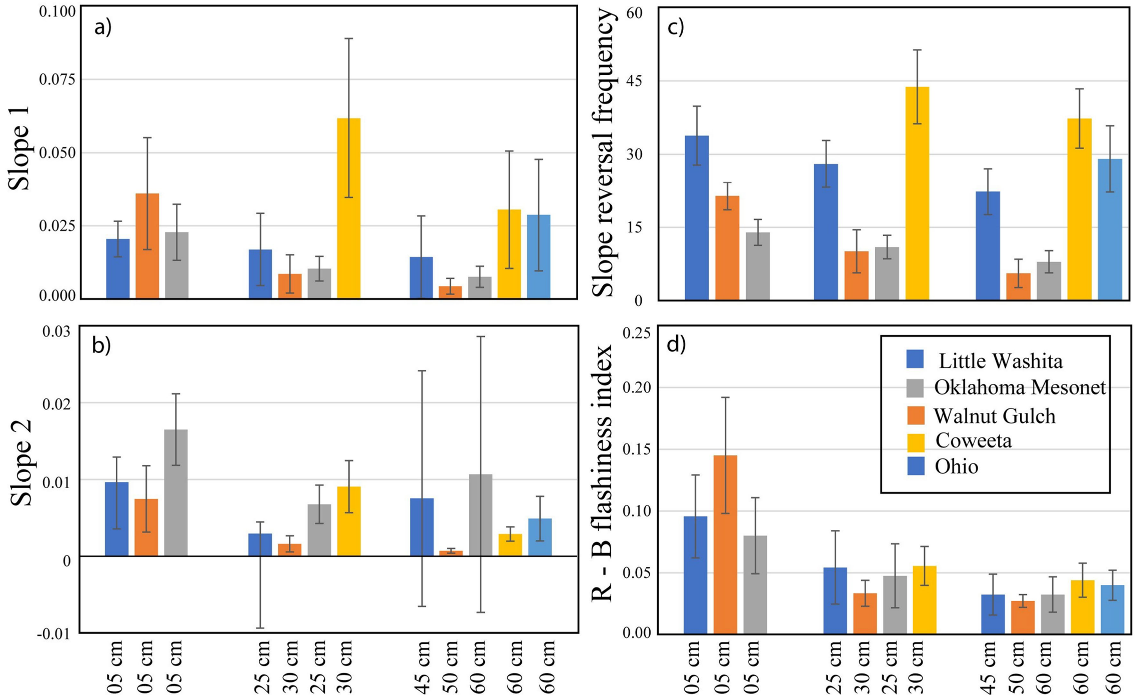

FIGURE 8
Site average of the soil moisture signatures for each depth. The colors indicate the sites with the *x*-axis showing the depths of observation time series and the *y*-axis: the computed signatures **(a)** slope 1, **(b)** slope 2, **(c)** slope reversal frequency, and **(d)** R-B flashiness index values.

across time further supports its utility as a diagnostic signature. Elevated surface flashiness is consistent with rapid wetting during precipitation events followed by rapid drying due to evaporation and near-surface drainage, whereas reduced flashiness at depth indicates progressive filtering of high-frequency signals within the soil profile. Interannual variability in flashiness differed across sites, highlighting the role of climatic variability in shaping near-surface soil moisture dynamics. For example, Little Washita, with its sub-humid continental climate and seasonally variable precipitation, exhibited pronounced interannual variability in flashiness, particularly in surface layers. In contrast, Walnut Gulch, constrained by semi-arid conditions and high evaporative demand than input rainfall, showed relatively stable and low flashiness values across years. These contrasting patterns are consistent with the known role of climate-driven variability in near-surface soil moisture dynamics (Seneviratne et al., 2010) and suggest that the adapted index responds coherently to climatic forcing across diverse environments. As with reversal frequency, flashiness integrates multiple interacting processes and should not be interpreted as a direct proxy for individual fluxes (Robinson et al., 2008; Vereecken et al., 2014).

Distinct site-specific behavior was also evident. The steep, forested Coweeta site exhibited high variability across time, depth, and space, whereas limited variability at Walnut Gulch reflects the constraints imposed by aridity (Figure 8). Similarly, relatively low variability at the Oklahoma Mesonet sites likely reflects limited topographic relief and the characteristics of heat dissipation sensors, which are known to be less responsive to rapid wetting events than electromagnetic sensors (Datta et al., 2018; Illston et al., 2008). These results emphasize that site-scale variability and depth-dependent behavior are more informative than spatial averaging when interpreting soil moisture dynamics, given the heterogeneity of soil properties, geomorphic settings, and cover conditions (Crow et al., 2012; Mohanty et al., 2017).

Vegetation and soil effects are expressed implicitly through their influence on evapotranspiration, infiltration, and storage, but were not explicitly parameterized in this study. Consequently, interpretations emphasize consistency with established hydrological understanding rather than direct process attribution. The proposed signatures should therefore be viewed as diagnostic indicators that summarize integrated system behavior rather than mechanistic representations.

The soil-moisture signatures presented here provide a comparative framework for diagnosing patterns in soil-moisture dynamics across depths and locations. Future research should leverage these metrics to disentangle the roles of static controls (e.g., soil texture, structure, porosity, and pedon-scale properties), temporal drivers (e.g., precipitation characteristics, antecedent moisture, and atmospheric demand), and geomorphic context (e.g., slope position, contributing area, and subsurface connectivity) in shaping soil-moisture behavior in space and time. Integrating these signatures with process-based and data-driven models offers a pathway to improve representation of infiltration, redistribution, and evapotranspiration processes across landscapes and climatic gradients.

Future research should focus on (1) standardizing soil-moisture data collection to improve comparability across sites, (2) expanding analyses to include a broader range of climatic and physiographic settings, and (3) integrating consistent pedon-level information to facilitate scaling from point measurements to landscape characterization. Addressing these needs will enhance the interpretability of soil-moisture signatures and broaden their applicability across observational networks and modeling frameworks.

A more comprehensive understanding of the spatial and temporal characteristics of soil-moisture dynamics, as summarized by these signatures, can contribute to improved assessment of runoff-generation potential, estimation of replenishable water for managed recharge, and interpretation of soil-moisture controls on ecosystem processes. Ultimately, these diagnostic metrics support land characterization and more informed land and water management by clarifying how climate, soil, and landscape position jointly shape soil-moisture behavior (Carrão et al., 2016; Kim, 2016; Vereecken et al., 2014; Verrot and Destouni, 2016).

Climate, particularly precipitation, acts as a primary discriminator in soil moisture dynamics by driving saturation and initiating wetting–drying cycles. However, the magnitude and variability of the three signatures reflect complex interactions among climate variables, soil properties, and geomorphic settings that cannot be fully disentangled from the current observational framework alone. Within-site variability underscores that local factors including soil texture, hydraulic conductivity, landscape position, and vegetation cover modulate how precipitation signals are transmitted, stored, and released through the soil profile. Quantifying the relative contributions of these interacting controls remains an open challenge, warranting dedicated investigation captures the nonlinear interactions across diverse environmental gradients.

Data availability statement

The original contributions presented in the study are included in the article/supplementary material, further inquiries can be directed to the corresponding author.

Author contributions

MM: Conceptualization, Data curation, Formal analysis, Investigation, Methodology, Project administration, Software, Validation, Visualization, Writing – original draft, Writing – review & editing. SR: Visualization, Writing – review & editing. BR: Conceptualization, Methodology, Writing – review & editing. MR: Writing – review & editing. CJ: Conceptualization, Formal analysis, Investigation, Methodology, Writing – review & editing.

Funding

The author(s) declared that financial support was not received for this work and/or its publication.

Acknowledgments

USDA is an equal opportunity provider, employer, and lender. Mention of a proprietary product does not constitute endorsement by USDA or the US government and does not imply its approval to the exclusion of the other products that may also be suitable.

Conflict of interest

The author(s) declared that this work was conducted in the absence of any commercial or financial relationships that could be construed as a potential conflict of interest.

Generative AI statement

The author(s) declared that Generative AI was not used in the creation of this manuscript.

Any alternative text (alt text) provided alongside figures in this article has been generated by Frontiers with the support of artificial intelligence and reasonable efforts have been made to ensure accuracy, including review by the authors wherever possible. If you identify any issues, please contact us.

Publisher's note

All claims expressed in this article are solely those of the authors and do not necessarily represent those of their affiliated organizations, or those of the publisher, the editors and the reviewers. Any product that may be evaluated in this article, or claim that may be made by its manufacturer, is not guaranteed or endorsed by the publisher.

References

Addor, N., Nearing, G., Prieto, C., Newman, A. J., Le Vine, N., and Clark, M. P. (2018). A ranking of hydrological signatures based on their predictability in space. *Water Resour. Res.* 54, 8792–8812. doi: 10.1029/2018WR022606

AghaKouchak, A., Farahmand, A., Melton, F. S., Teixeira, J., Anderson, M. C., Wardlow, B. D., et al. (2015). Remote sensing of drought: Progress, challenges and opportunities. *Rev. Geophys.* 53, 452–480.

Araki, R., Branger, F., Wiekenkamp, I., and McMillan, H. (2022). A signature-based approach to quantify soil moisture dynamics under contrasting land-uses. *Hydrol. Process.* 36:e14553. doi: 10.1002/hyp.14553

Baker, D. B., Richards, R. P., Loftus, T. T., and Kramer, J. W. (2004). A new flashiness index: Characteristics and applications to midwestern rivers and streams 1. *JAWRA* 40, 503–522. doi: 10.1111/j.1752-1688.2004.tb01046.x

Basara, J. B., and Crawford, T. M. (2000). Improved installation procedures for deep-layer soil moisture measurements. *J. Atmos. Ocean. Technol.* 17, 879–884. doi: 10.1175/1520-0426(2000)017<0879:iipfdl>2.0.co;2

Branger, F., and McMillan, H. K. (2020). Deriving hydrological signatures from soil moisture data. *Hydrol. Process.* 34, 1410–1427. doi: 10.1002/hyp.13645

Brocca, L., Morbidelli, R., Melone, F., and Moramarco, T. (2007). Soil moisture spatial variability in experimental areas of central Italy. *J. Hydrol.* 333, 356–373. doi: 10.1016/j.jhydrol.2006.09.004

Brutsaert, W. (2008). Long-term groundwater storage trends estimated from streamflow records: Climatic perspective. *Water Resour. Res.* 44:6518. doi: 10.1029/2007WR006518

Buchanan, B., Fleming, M., Schneider, R., Richards, B., Archibald, J., Qiu, Z., et al. (2014). Evaluating topographic wetness indices across central new york agricultural landscapes. *Hydrol. Earth Syst. Sci.* 18, 3279–3299. doi: 10.5194/hess-18-3279-2014

Carra˜o, H., Russo, S., Sepulcre-Canto, G., and Barbosa, P. (2016). An empirical stan- dardized soil moisture index for agricultural drought assessment from remotely sensed data. *Int. J. Appl. Earth Obs. Geoinf.* 48, 74–84. doi: 10.1016/j.jag.2015.06.011

Collison, E., Riutta, T., and Slade, E. M. (2013). Macrofauna assemblage composition and soil moisture interact to affect soil ecosystem functions. *Acta Oecol.* 47, 30–36. doi: 10.1016/j.actao.2012.12.002

Cook, D. R. (2016). *Soil Water and Temperature System (SWATS) instrument handbook*. Oak Ridge, TN: Office of Scientific and Technical Information (OSTI).

Corradini, C. (2014). Soil moisture in the development of hydrological processes and its determination at different spatial scales. *J. Hydrol.* 516, 1–5. doi: 10.1016/j.jhydrol.2014.02.051

Cosh, M. H., Jackson, T. J., Starks, P., and Heathman, G. (2006). Temporal stability of surface soil moisture in the little washita river watershed and its applications in satellite soil moisture product validation. *J. Hydrol.* 323, 168–177. doi: 10.1016/j.jhydrol.2005.08.020

Crow, W. T., Berg, A. A., Cosh, M. H., Loew, A., Mohanty, B. P., and Panciera, R. (2012). Upscaling sparse ground-based soil moisture observations for the validation of coarse-resolution satellite soil moisture products. *Geophysics* 50:372. doi: 10.1029/2011RG000372

D'Odorico, P., Laio, F., Porporato, A., Ridolfi, L., Rinaldo, A., and Rodriguez-Iturbe, I. (2010). Ecohydrology of terrestrial ecosystems. *Bioscience* 60, 898–907. doi: 10.1525/bio.2010.60.11.6

Datta, S., Taghvaeian, S., Ochsner, T., Moriasi, D., Gowda, P., and Steiner, J. (2018). Performance assessment of five different soil moisture sensors under irrigated field conditions in Oklahoma. *Sensors* 18:3786. doi: 10.3390/s18113786

Dyer, J. M. (2006). Revisiting the deciduous forests of eastern north America. *Bioscience* 56, 341–352. doi: 10.1641/0006-3568(2006)56[341:RTDFOE]2.0.CO;2

Dyer, J. M. (2009). Assessing topographic patterns in moisture use and stress using a water balance approach. *Landsc. Ecol.* 24, 391–403. doi: 10.1007/s10980-008-9316-6

Entekhabi, D., Rodriguez-Iturbe, I., and Castelli, F. (1996). Mutual interaction of soil moisture state and atmospheric processes. *J. Hydrol.* 184, 3–17. doi: 10.1016/0022-1694(95)02965-6

Famiglietti, J. S., Ryu, D., Berg, A. A., Rodell, M., and Jackson, T. J. (2008). Field observations of soil moisture variability across scales. *Water Resour. Res.* 44:804. doi: 10.1029/2006WR005804

Fern'andez-Long, M. E., Peretti, M., Carnelos, D., Della-Chiesa, T., and Spescha, L. (2021). Characterization of the seasonal variation of soil moisture in Argentina. *Internat. J. Climatol.* 41, E537–E547. doi: 10.1002/joc.6705

Garcıa, G. M., Pachepsky, Y. A., and Vereecken, H. (2014). Effect of soil hydraulic properties on the relationship between the spatial mean and variability of soil moisture. *J. Hydrol.* 516, 154–160.

Goodrich, D., Unkrich, C., Keefer, T., Nichols, M., Stone, J., Levick, L., et al. (2008). Event to multidecadal persistence in rainfall and runoff in southeast arizona. *Water Resour. Res.* 44. doi: 10.1029/2007WR006222

Grabs, T., Seibert, J., Bishop, K., and Laudon, H. (2009). Modeling spatial patterns of saturated areas: A comparison of the topographic wetness index and a dynamic distributed model. *J. Hydrol.* 373, 15–23. doi: 10.1016/j.jhydrol.2009.03.031

Grayson, R. B., Western, A. W., Chiew, F. H., and Blöschl, G. (1997). Preferred states in spatial soil moisture patterns: Local and nonlocal controls. *Water Resour. Res.* 33, 2897–2908. doi: 10.1029/97WR02174

Hales, T. C., and Miniat, C. F. (2017). Soil moisture causes dynamic adjustments to root reinforcement that reduce slope stability. *Earth Surf. Process. Landf.* 42, 803–813. doi: 10.1002/esp.4039

Hamerlynck, E. P., Scott, R. L., and Stone, J. J. (2012). Soil moisture and ecosys- tem function responses of desert grassland varying in vegetative cover to a saturating precipitation pulse. *Ecohydrology* 5, 297–305. doi: 10.1002/eco.214

Hatfield, J. L., Sauer, T. J., and Prueger, J. H. (2001). Managing soils to achieve greater water use efficiency: a review. *Agron. J.* 93, 271–280. doi: 10.2134/agronj2001.932271x

Heathman, G. C., Starks, P. J., Ahuja, L. R., and Jackson, T. J. (2003). Assimilation of Surface Soil Moisture to Estimate Profile Soil Water Content. *J. Hydrol.* 284, 54–68. doi: 10.1016/S0022-1694(03)00243-1

Heilman, P., Nichols, M., Goodrich, D., Miller, S., and Guertin, D. (2008). Geographic information systems database, walnut gulch experimental watershed, Arizona, united states. *Water Resour. Res.* 44:777. doi: 10.1029/2006WR005777

Hewlett, J. D., and Hibbert, A. R. (1963). Moisture and Energy Conditions within a Sloping Soil Mass during Drainage. *J. Geophys. Res.* 68, 1081–1087. doi: 10.1029/JZ068i004p01081

Holden, Z. A., Swanson, A. K., Sadegh, M., Luce, C. H., Noonan-Wright, E., and Parsons, R. A. (2025). Soil moisture is a stronger predictor of forest fire spread potential than weather in the US Northern Rocky Mountains. *Geophys. Res. Lett.* 52:e2025GL116248. doi: 10.1029/2025GL116248

Illston, B. G., Basara, J. B., Fiebrich, C. A., Crawford, K. C., Hunt, E., Fisher, D. K., et al. (2008). Mesoscale monitoring of soil moisture across a statewide network. *J. Atmos. Ocean. Technol.* 25, 167–182. doi: 10.1175/2007jtecha993.1

Kathuria, D., Mohanty, B. P., and Katzfuss, M. (2019). A nonstationary geostatistical framework for soil moisture prediction in the presence of surface heterogeneity. *Water Resour. Res.* 55, 729–753. doi: 10.1029/2018WR023505

Kim, S. (2009). Characterization of soil moisture responses on a hillslope to sequential rainfall events during late autumn and spring. *Water Resour. Res.* 45:7239. doi: 10.1029/2008WR007239

Kim, S. (2016). Time series modeling of soil moisture dynamics on a steep mountainous hillside. *J. Hydrol.* 536, 37–49. doi: 10.1016/j.jhydrol.2016.02.027

Kopecký, M., Macek, M., and Wild, J. (2021). Topographic wetness index calculation guidelines based on measured soil moisture and plant species composition. *Sci. Total Environ.* 757:143785. doi: 10.1016/j.scitotenv.2020.143785

Koster, R. D., Dirmeyer, P. A., Guo, Z., Bonan, G., Chan, E., Cox, P., et al. (2004). Regions of strong coupling between soil moisture and precipitation. *Science* 305, 1138–1140. doi: 10.1126/science.1100217

Koster, R. D., Mahanama, S. P., Livneh, B., Lettenmaier, D. P., and Reichle, R. H. (2010). Skill in streamflow forecasts derived from large-scale estimates of soil moisture and snow. *Nat. Geosci.* 3, 613–616. doi: 10.1038/ngeo944

Larson, J., Lidberg, W., Agren, A. M., and Laudon, H. (2022). Predicting soil moisture conditions across a heterogeneous boreal catchment using terrain indices. *Hydrol. Earth Syst. Sci.* 26, 4837–4851. doi: 10.5194/hess-26-4837-2022

Löffler, J. (2007). The influence of micro-climate, snow cover, and soil moisture on ecosystem functioning in high mountains. *J. Geogr. Sci.* 17, 3–19. doi: 10.1007/s11442-007-0003-3

McColl, K. A., Alemohammad, S. H., Akbar, R., Konings, A. G., Yueh, S., and En-tekhabi, D. (2017). The global distribution and dynamics of surface soil moisture. *Nat. Geosci.* 10, 100–104. doi: 10.1038/ngeo2868

McPherson, R. A., Fiebrich, C. A., Crawford, K. C., Kilby, J. R., Grimsley, D. L., Martinez, J. E., et al. (2007). Statewide monitoring of the mesoscale environment: A technical update on the Oklahoma Mesonet. *J. Atmos. Ocean. Technol.* 24, 301–321. doi: 10.1175/JTECH1976.1

Meles, M. B., Younger, S. E., Jackson, C. R., Du, E., and Drover, D. (2020). Wetness index based on landscape position and topography (wilt): Modifying twi to reflect landscape position. *J. Environ. Manag.* 255:109863. doi: 10.1016/j.jenvman.2019.109863

Mimeau, L., Tramblay, Y., Brocca, L., Massari, C., Camici, S., and Finaud-Guyot, P. (2021). Modeling the response of soil moisture to climate variability in the mediter- ranean region. *Hydrol. Earth Syst. Sci.* 25, 653–669. doi: 10.5194/hess-25-653-2021

Mittelbach, H., and Seneviratne, S. I. (2012). A new perspective on the spatio-temporal variability of soil moisture: temporal dynamics versus time-invariant contributions. *Hydrol. Earth Syst. Sci.* 16, 2169–2179. doi: 10.5194/hess-16-2169-2012

Mohanty, B. P., Cosh, M. H., Lakshmi, V., and Montzka, C. (2017). Soil moisture remote sensing: State-of-the-science. *Vadose Zone J.* 16, 1–9. doi: 10.2136/vzj2016.10.0105

Molden, D., Oweis, T., Steduto, P., Bindraban, P., Hanjra, M. A., and Kijne, J. (2010). Improving agricultural water productivity: Between optimism and caution. *Agric. Water Manage.* 97, 528–535. doi: 10.1016/j.agwat.2009.03.023

Moran, M., Holifield Collins, C., Goodrich, D. C., Qi, J., Shannon, D., and Olsson, A. (2008). Long-term remote sensing database, walnut gulch experimental watershed, arizona, united states. *Water Resour. Res.* 44:5689. doi: 10.1029/2006WR005689

Penna, D., Brocca, L., Borga, M., and Dalla Fontana, G. (2013). Soil moisture temporal stability at different depths on two alpine hillslopes during wet and dry periods. *J. Hydrol.* 477, 55–71. doi: 10.1016/j.jhydrol.2012.10.052

Radu-la, M. W., Szymura, T. H., and Szymura, M. (2018). Topographic wetness in- dex explains soil moisture better than bioindication with ellenberg's indicator values. *Ecol. Indic.* 85, 172–179. doi: 10.1016/j.ecolind.2017.10.011

Rahman, M., Solis, S. S., Harter, T., Saeedimoghaddam, M., Efron, N., and Nearing, G. S. (2024). Drought awareness over continental united states. *J. Hydrol.* 22:131868.

Riihimäki, H., Kemppinen, J., Kopeckỳ, M., and Luoto, M. (2021). Topographic wetness index as a proxy for soil moisture: The importance of flow-routing algorithm and grid resolution. *Water Resour. Res.* 57:871. doi: 10.1029/2021WR029871

Robinson, D. A., Campbell, C. S., Hopmans, J. W., Hornbuckle, B. K., Jones, S. B., Knight, R., et al. (2008). Soil moisture measurement for ecological and hydrological watershed-scale observatories: A review. *Vadose Zone J.* 7, 358–389. doi: 10.2136/vzj2007.0143

Rodrıguez-Iturbe, I., and Porporato, A. (2007). *Ecohydrology of water-controlled ecosystems: soil moisture and plant dynamics*. Cambridge: Cambridge University Press.

Scott, B. L., Ochsner, T. E., Illston, B. G., Fiebrich, C. A., Basara, J. B., and Sutherland, A. J. (2013). New soil property database improves Oklahoma Mesonet soil moisture estimates. *J. Atmos. Ocean. Technol.* 30, 2585–2595. doi: 10.1175/jtech-d-13-00084.1

Seneviratne, S. I., Corti, T., Davin, E. L., Hirschi, M., Jaeger, E. B., Lehner, I., et al. (2010). Investigating soil moisture–climate interactions in a changing climate: A review. *Earth Sci. Rev.* 99, 125–161. doi: 10.1016/j.earscirev.2010.02.004

Seneviratne, S. I., Wilhelm, M., Stanelle, T., van den Hurk, B., Hagemann, S., Berg, A., et al. (2013). Impact of soil moisture-climate feedbacks on cmip5 projections: First results from the glace-cmip5 experiment. *Geophys. Res. Lett.* 40, 5212–5217. doi: 10.1002/grl.50956

Sheffield, J., Wood, E. F., and Roderick, M. L. (2012). Little change in global drought over the past 60 years. *Nature* 491, 435–438. doi: 10.1038/nature11575

Shellito, P. J., Small, E. E., Colliander, A., Bindlish, R., Cosh, M. H., Berg, A. A., et al. (2016). SMAP soil moisture drying more rapid than observed in situ following rainfall events. *Geophys. Res. Lett.* 43, 8068–8075.

Sörensen, R., Zinko, U., and Seibert, J. (2006). On the calculation of the topographic wetness index: evaluation of different methods based on field observations. *Hydrol. Earth Syst. Sci.* 10, 101–112. doi: 10.5194/hess-10-101-2006

Starks, P. J., Heathman, G. C., Jackson, T. J., and Cosh, M. H. (2014b). Upper Washita River Experimental Watersheds: Multiyear Stability of Soil Water Content Profiles. *Agric. Water Manag.* 147, 135–143. doi: 10.1016/j.agwat.2014.05.018

Starks, P. J., Steiner, J. L., and Stern, A. J. (2014a). Upper Washita river experimental watershed: Land cover data sets (1974–2007) for two southwestern Oklahoma agricultural watersheds. *J. Environ. Qual.* 43, 1310–1318. doi: 10.2134/jeq2013.07.0292

Teuling, A. J., Hupet, F., Uijlenhoet, R., and Troch, P. A. (2007). Climate variability effects on spatial soil moisture dynamics. *Geophys. Res. Lett.* 34:9080. doi: 10.1029/2006GL029080

Tso, C.-H. M., Blyth, E., Tanguy, M., Levy, P. E., Robinson, E. L., Bell, V., et al. (2023). Multiproduct characterization of surface soil moisturedrydowns in the United Kingdom. *J. Hydrometeorol.* 24, 2299–2319. doi: 10.1175/JHM-D-23-0018.1

USDA NRCS (2019). Soil Survey of Macon County, North Carolina. USDA, USA.

Vereecken, H., Huisman, J., Bogena, H., Vanderborght, J., Vrugt, J., and Hopmans, J. (2008). On the value of soil moisture measurements in vadose zone hydrology: A review. *Water Resour. Res.* 44:6829. doi: 10.1029/2008WR006829

Vereecken, H., Huisman, J., Pachepsky, Y., Montzka, C., Van Der Kruk, J., Bogena, H., et al. (2014). On the spatio-temporal dynamics of soil moisture at the field scale. *J. Hydrol.* 516, 76–96. doi: 10.1016/j.jhydrol.2013.11.061

Verrot, L., and Destouni, G. (2016). Data-model comparison of temporal variability in long-term time series of large-scale soil moisture. *J. Geophys. Res. Atmos.* 516, 76–96. doi: 10.1016/j.jhydrol.2013.11.061

Western, A. W., Zhou, S.-L., Grayson, R. B., McMahon, T. A., Blöschl, G., Wilson, D. J., et al. (2004). Spatial correlation of soil moisture in small catchments and its relationship to dominant spatial hydrological processes. *J. Hydrol.* 286, 113–134.

Wilson, D. J., Western, A. W., and Grayson, R. B. (2004). Identifying and quantify- ing sources of variability in temporal and spatial soil moisture observations. *Water Resour. Res.* 40:2306. doi: 10.1029/2003WR002306

Xu, Y., Dong, K., Jiang, M., Liu, Y., He, L., Wang, J., et al. (2022). Soil moisture and species richness interactively affect multiple ecosystem functions in a microcosm experiment of simulated shrub encroached grasslands. *Sci. Total Environ.* 803:149950. doi: 10.1016/j.scitotenv.2021.149950